Critical nucleation size of vortex core for domain wall transformation in soft magnetic thin film nanostrips

Youn-Seok Choi, Jun-Young Lee, Myoung-Woo Yoo, Ki-Suk Lee, Konstantin Yu. Guslienko,* and Sang-Koog Kim†
Department of Materials Science and Engineering, Research Center for Spin Dynamics and Spin-Wave Devices, Nanospinics Laboratory, Research Institutes of Advanced Materials, Seoul National University, Seoul 151-744, Republic of Korea
(Received 1 April 2009; published 7 July 2009)

We have studied the onset process of dynamic transformation of the internal structure of a moving domain wall (DW) in soft magnetic thin film nanostrips, driven by applied magnetic fields larger than the Walker field strength, H_w. It was found that one of the edge-soliton cores of a transverse wall (TW)-type DW should reach a critical nucleation size of the vortex core by moving inward beyond a critical deviation, Δy_{cri}, in the transverse (width) direction, in order for the transformation from a TW to a vortex wall (VW) (or antivortex wall, AVW) to occur. The value of Δy_{cri} is estimated to be close to the full width at half maximum of the out-of-plane magnetizations of a stabilized vortex core (or antivortex core). Upon completion of the nucleation of the vortex (antivortex) core, the VW (AVW) is stabilized, accompanying its characteristic gyrotropic motion in a potential well (hill) of a given nanostrip. Field strengths exceeding the H_w, the onset field of DW velocity breakdown, are not sufficient but necessary conditions for the dynamic DW transformations.

DOI: 10.1103/PhysRevB.80.012402 PACS number(s): 75.60.Ch, 75.70.Kw, 75.75.+a

Numerous recent studies in the fields of nanomagnetism and magnetization (**M**) dynamics have focused on magnetic field and/or current driven dynamic motions of domain walls (DWs) in patterned magnetic thin film nanostrips,[1–7] owing to the potential applications to solid-state data storage and logic devices.[8–14] One of the most fundamental issues in this field is the underlying physics of the breakdown of DW velocity and oscillatory DW motions under magnetic fields exceeding a threshold field known as the Walker field, H_w. This question has been approached by Walker,[15] Thiaville *et al.*,[16] and Nakatani *et al.*[3] within the context of one-dimensional (1D) models. These 1D models, however, can partially explain the linear increases of DW velocity with the field strength in a low-field regime, as well as the Walker breakdown behaviors in an intermediate-field regime.

Alternatively, two-dimensional (2D) dynamic soliton models recently developed by Lee *et al.*,[17] Tretiakov *et al.*,[18,19] and Guslienko *et al.*[20] have begun to render general explanations of the DW dynamics in the low-field and intermediate-field regimes with reference to the dynamic transformation of the internal structure of a moving DW between transverse wall (TW) and antivortex wall (AVW) or vortex wall (VW). According to these 2D models, dynamic transformations are just the results of serial processes of the nucleation (emission), gyrotropic motion (propagation), and annihilation (absorption) of topological solitons such as vortex (V) or antivortex (AV) with the conservation of total topological charges inside a given nanostrip.[17–20] In addition, DW dynamics and its related **M** reversals under higher magnetic fields beyond the Walker breakdown regime can be explained through the nucleation and annihilation of the V-AV pairs.[21–23]

Although such nontrivial novel DW dynamic behaviors in patterned nanostrips can be learned in the context of the 2D dynamic soliton models and/or 1D model developed thus far, the onset process of the dynamic transformation of the TW to the VW (or AVW) have yet been clarified. In this Brief Report, we present the results of a study on the dynamic process of the nucleation of, e.g., a VW for DW transformation, and also suggest a simple way to manipulate the transformation to avoid the reduction (breakdown) in DW velocities above the H_w.

In the present micromagnetic calculations, we used Permalloy ($Py:Ni_{80}Fe_{20}$) thin film nanostrips of rectangular cross section, and 10 nm thickness, 200 nm width, and 6.0 μm length as illustrated in Fig. 1(a). The material parameters chosen were as follows: the saturation magnetization $M_s=8.6\times10^5$ A/m and the exchange stiffness $A_{ex}=1.3\times10^{-11}$ J/m with zero magnetocrystalline anisotropy. To examine the **M** dynamics of individual cells of $2.5\times2.5\times10$ nm^3 with the Gilbert damping constant of $\alpha=0.01$, we used the OOMMF code[24] that employs the Landau-Lifshitz-Gilbert equation of **M** motion.[25] As shown in Fig. 1(a), we started with a head-to-head TW-type DW (of net **M** in the $+y$ direction), which DW was positioned in the middle of the long axis of a given nanostrip. The TW motion was

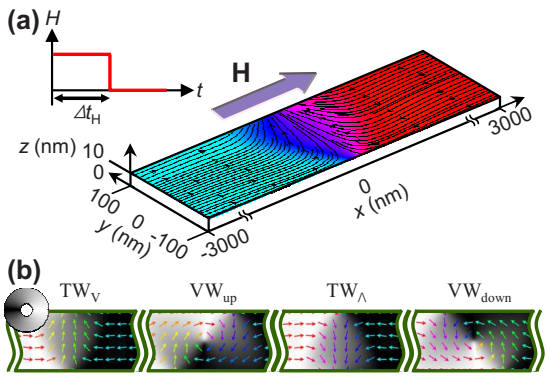

FIG. 1. (Color online) (a) Thin film Py nanostrip of the indicated dimensions along with the initial **M** configuration of a TW-type DW placed in the middle of long axis. The in-plane orientations of the local **M**s are represented by the colors and streamlines. The inset shows a step-pulse field with duration time Δt_H. (b) Plane-view snapshot images of dynamic transformation of moving DWs driven by a static field $H=35$ Oe. The small arrows and the black and white colors in the wheel indicate the local in-plane **M** orientations.

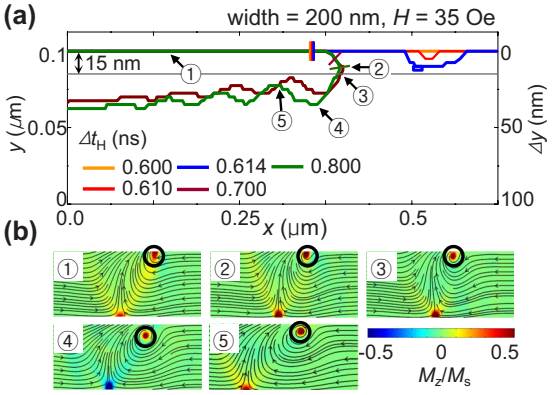

FIG. 2. (Color online) (a) Trajectories of moving edge-soliton cores placed initially at the upper edge in nanostrips under applied step-pulse fields with the indicated values of Δt_H. The small vertical lines on the trajectories correspond to the times at which the pulse fields were turned off in each case. (b) Plane-view snapshot images of those temporal evolutions taken at times marked by the small arrows with numbers on the trajectory for the case of $\Delta t_H = 0.800$ ns.

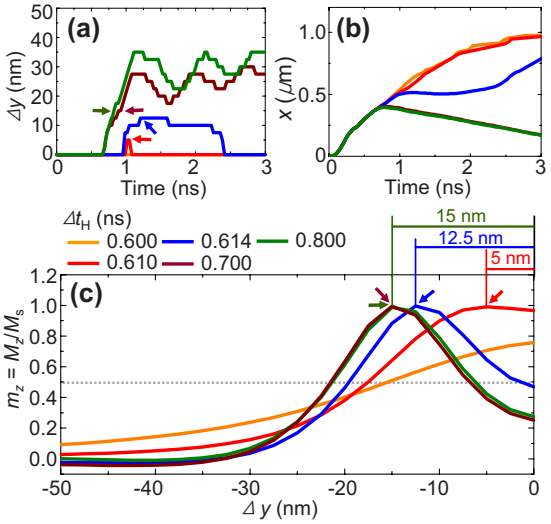

FIG. 3. (Color online) (a) Transverse displacement, Δy, from the upper edge and (b) longitudinal (x) displacement of the position of the upper-edge-soliton core for each case of Δt_H's shown in Fig. 2(a). (c) m_z profiles along the transverse direction across the upper-edge-soliton core, taken at the times described in the text. The dotted horizontal line corresponds to $m_z = 1/2$.

driven by H applied in the $+x$ direction. We chose field strengths greater than the H_w, which are necessary for the transformation of the TW to either the VW or AVW, as shown from earlier studies.[17,21,26,27] For example, the dynamic transformation of the internal structure of a moving DW under a static field of $H=35$ Oe is illustrated by snapshot images representing the serial changes from $TW_V \rightarrow VW_{up} \rightarrow TW_\Lambda \rightarrow VW_{down}$ (where the subscripts indicate the soliton core polarization) [Fig. 1(b)]. For $H > H_w$, such DW internal structural changes take place but different types of structural changes can be observed for the different H strengths and the dimensions of a given nanostrip.[17] For $H < H_w$, however, such DW transformations never occur and the TW rather shows a steady movement along nanostrips while its edge-soliton cores are kept in the same or similar relative positions. Thus, the H_w is known to be the onset field above which the dynamic changes in the internal DW structure occur.

To clarify the onset processes of such transformations, we studied the nucleation process of a V (AV) at strip edges, i.e., the stabilization process of a VW (AVW). To do so, in place of static fields, we used applications of single-step-pulse fields with different duration times Δt_H and with an equal field strength $H=35$ Oe $> H_w$, as illustrated in the inset of Fig. 1(a). Here, we chose a specific transformation, for example, $TW_V \rightarrow VW_{up}$, which is a part of the internal structural change in the unit period of $TW_V \rightarrow VW_{up} \rightarrow TW_\Lambda \rightarrow VW_{down}$ [Fig. 1(b)], namely, the type (ii) indicated in Ref. 17. The VW-type DW has a parabolic potential *well* along the width direction, and hence, when a moving TW turns into a VW, the forward motion of the TW turns into the backward motion of the VW-type DW. Accordingly, the onset of DW transformations can be determined by examining the change in the longitudinal direction of DW motions.

Figure 2(a) shows the position trajectories of the upper-edge-soliton core in motion driven by each of step-pulse fields, $\Delta t_H = 0.600$, 0.610, 0.614, 0.700, and 0.800 ns with $H=35$ Oe. For the relatively short durations, $\Delta t_H = 0.600$, 0.610, and 0.614 ns, the TW_V generally maintained its original overall structure and moved along the long axis of the nanostrip. Even after the pulse fields were turned off (those times were marked with small lines on the trajectories), the upper-edge-soliton core of the TW moved inward slightly but immediately returned to the upper edge, as shown in those trajectories. Thus, under these conditions the DW in its whole motion is the TW type in the **M** configuration. In contrast, for the relatively long pulse durations, $\Delta t_H = 0.700$ and 0.800 ns, the TW was changed in shape irreversibly to the VW-type DW, after it started to move backward in the longitudinal direction and moved farther from the upper edge in the transverse direction [see the small circles on the serial snapshot images in Fig. 2(b)]. The transverse oscillatory motions may be caused by interactions between the newly nucleated vortex core near the upper edge and the edge-soliton core (initially placed at the bottom edge) experiencing its polarization reversal. See the change in the polarization of the bottom edge core on the images with indicated numbers, ③, ④, and ⑤ in Fig. 2(b).

It is difficult to explain such contrasting DW motions between the longer and shorter durations with equal strength $H=35$ Oe larger than H_w in the context of the already developed 1D models. To understand those contrasting behaviors more quantitatively, we plotted the position deviations, Δy, of the upper-edge-soliton core in the transverse direction from the upper edge [Fig. 3(a)], as well as its longitudinal displacements [Fig. 3(b)]. For the upper-edge-soliton core that moves within 12.5 nm in the transverse direction from the upper edge, the core immediately returns to the upper edge again and it moves farther toward the $+x$ direction, without any DW transformations. On the contrary, for the cases where the upper-edge-soliton core [shown by snapshot images for $\Delta t_H = 0.800$ ns in Fig. 2(b)] moves beyond a de-

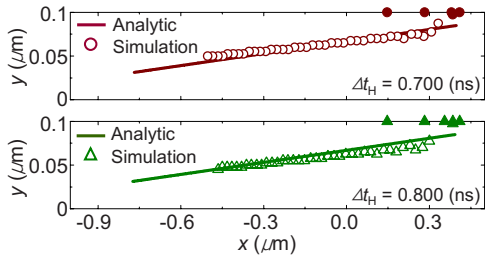

FIG. 4. (Color online) Trajectories of the backward motion of the upper-edge-soliton core after it was nucleated and stabilized (open symbols), initially driven by step-pulse fields of Δt_H=0.700 and 0.800 ns, and the calculation results of an analytical equation of soliton-core trajectories obtained based on the 2D dynamic soliton model (solid line). The backward motions were obtained for much longer times than Δt_H. The solid symbols correspond to the trajectories of the TW-type DW before its transformation to the VW-type DW.

viation of 15 nm in the transverse direction, the forward motion in the longitudinal direction turns into a backward motion, as in the characteristic gyrotropic motion of the "vortex core" in a given potential well.[28]

From the above results, we conclude that there exists a critical transverse deviation of the vortex core position from the strip edge, Δy_{cri}, that determines the onset of the backward motion of the TW in the longitudinal direction, and hence yielding the transformation of the TW-type to VW-type DW. In this study, the value of Δy_{cri} is estimated to be larger than 12.5 nm and less than 15.0 nm, according to the m_z (M_z/M_s) profiles of the upper-edge core, taken when the Δy values are maximum for Δt_H=0.600, 0.610, and 0.614 or when the Δy values reach 15 nm for Δt_H=0.700 and 0.800, as shown in Fig. 3(c). The value of $12.5 < \Delta y_{cri}(\text{nm}) < 15.0$ is close to the full width at half maximum (FWHM) of the m_z profile, Δw_{FWHM}=14 nm, for a stabilized vortex core in a circular dot of 200 nm diameter and 10 nm thickness. This result indicates that the VW can be stabilized when its core position moves inward sufficiently to Δw_{FWHM}=14 nm in the transverse direction. Consequently, in order for the process of transformation from a TW to VW (or AVW) to occur, an edge-soliton core of the TW-type DW should grow sufficiently to Δw_{FWHM}=14 nm. Upon Δy reaching Δy_{cri}, the edge-soliton core satisfies its critical nucleation size required to become a vortex core for DW transformation in soft magnetic thin film nanostrips. After then, once the VW (AVW) is stabilized, its core accompanies the gyrotropic motion in a potential well (hill) of a given nanostrip.

The critical nucleation size mentioned above is associated closely with an intrinsic core size that is determined by only the intrinsic material parameters of a given constituent material, here Py. Thus, Δy_{cri} is independent of any external driving force parameters, as confirmed by additional simulations with different pulse amplitudes. However, the geometry and dimension parameters of a confined nanodot sample can affect the intrinsic core size through the dipolar interaction, as calculated from $\Delta w_{FWHM}=0.68L_e(L/L_e)^{1/3}$ with the thickness L of a dot and the exchange length L_e.[29] The estimated value from the equation is about 10 nm, which is smaller than Δw_{FWHM}=14 nm estimated from the present simulations. This is consistent with the fact that the analytically calculated values are typically smaller than the simulation and experimental results.[30]

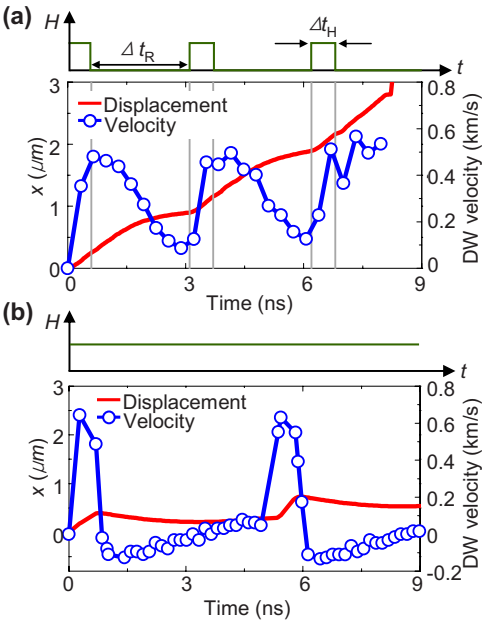

FIG. 5. (Color online) Longitudinal (x) displacements and velocities of DW motions driven by a periodic step-pulse field with H=35 Oe and with Δt_H=0.600 ns, Δt_R=2.5 ns in (a) and by a static field of H=35 Oe in (b).

In addition, it is worthwhile to emphasize the role of the Walker field in DW transformations. The Walker field is known to be the onset field above which the breakdown of DW velocities occurs, leading to oscillatory backward and forward motions of a DW in nanostrips. However, on the basis of this study, the applied magnetic fields exceeding the H_w are not the sufficient condition but rather a necessary condition required for the dynamic changes in a TW to either VW or AVW. In order for such DW transformations to occur, the cores of the edge soliton injected or nucleated from the edges should reach its critical nucleation size for stabilizing a newly formed V or AV. Thus, the core position of the newly nucleated V or AV should reach beyond $\Delta y_{cri} \sim 14$ nm for DW transformations. This result also reflects the fact that 2D dynamic soliton models of DW dynamics are more suitable than 1D models for interpreting and understanding the internal structural changes in moving DWs above the H_w.

To confirm the applicability of 2D soliton models for the interpretation of the nucleation process of VW or AVW, we also compared the simulation results of the trajectory of the backward motion of a vortex core after it was nucleated and stabilized and the numerical calculation of an analytical equation derived using the 2D dynamic soliton model.[20] After the nucleation of the vortex core, its motion was driven without applications of pulse fields, H=0. The trajectories of the vortex-core backward motion[31] can thus be obtained by inputting H=0 into the parabolic trajectory equation for a certain field $H > H_w$, described in Ref. 20 such that $Y(t) - Y(0) = (1/C)[X(t) - X(0)]$. The $X(t)$ and $Y(t)$ correspond to the x and y components of the soliton core position. We chose the value of $[X(0), Y(0)]$ as the core position at which

the vortex core starts to move backward in the x direction. The trajectory slope, $[Y(t)-Y(0)]/[X(t)-X(0)]$ is thus simply given as $1/C$. For the geometry and dimensions of the given Py nanostrip, the value of C was estimated to be 21.71,[20] which is in quantitative agreement with the simulation results shown in Fig. 4.

The dynamical process of the nucleation of a vortex core near strip edges is an important factor from an application perspective. According to the above results, periodic pulse fields can be implemented to manipulate the internal structure of a moving DW, in particular, in order to avoid the DW transformation that yields the velocity breakdown above the H_w. Figure 5 shows an example of the overall DW motion driven by a periodic pulse field with $H=35$ Oe$>H_w$ and duration time $\Delta t_H=0.6$ ns and accompanying relaxation time $\Delta t_R=2.5$ ns, compared with those driven by a static field of $H=35$ Oe. For the case of the static field, the DW internal structure changes, as already shown in Fig. 1(b), thus the different DW structures show their characteristic motions, yielding the overall oscillatory behavior of the longitudinal displacement and velocity. In contrast, the periodic pulse field does not allow the TW-to-VW transformation [Fig. 5(b)]. The average velocity of the TW is estimated to be 350 m/s, which is 4.7 times greater than the average velocity of 75 m/s in the oscillatory DW motion driven by the static field. It is worthwhile to note that the application of such periodic pulse fields offers an efficient way to prohibit the breakdown (reduction) of DW velocities above the H_w, without using the rough edge of a given nanostrip,[3] an underlayer of strong perpendicular magnetization,[27] and the application of perpendicular magnetic fields.[32]

In conclusion, the present study on the nucleation of a vortex core driven by step-pulse fields offers a physical explanation of the onset process of domain wall dynamic transformations observed experimentally, as well as a simple way to control the domain wall velocity breakdown typically observed above the Walker field.

This work was supported by Basic Science Research Program through the National Research Foundation of Korea (NRF) funded by the Ministry of Education, Science and Technology (No. 20090063589).

*Present address: Departamento de Fisica de materiales, Universidad del Pais Vasco, 20018 Donostia-San Sebastian, Spain.
†Corresponding author; sangkoog@snu.ac.kr

[1] A. A. Thiele, J. Appl. Phys. **45**, 377 (1974).
[2] R. Cowburn and D. Petit, Nature Mater. **4**, 721 (2005).
[3] Y. Nakatani, A. Thiaville, and J. Miltat, Nature Mater. **2**, 521 (2003).
[4] D. Atkinson *et al.*, Nature Mater. **2**, 85 (2003).
[5] G. S. D. Beach, C. Nistor, C. Knutson, M. Tsoi, and J. L. Erskine, Nature Mater. **4**, 741 (2005).
[6] L. Thomas *et al.*, Appl. Phys. Lett. **87**, 262501 (2005).
[7] L. Thomas, M. Hayashi, X. Jiang, R. Moriya, C. Rettner, and S. S. P. Parkin, Nature **443**, 197 (2006); A. Kunz, J. Appl. Phys. **99**, 08G107 (2006).
[8] M. Kläui, P.-O. Jubert, R. Allenspach, A. Bischof, J. A. C. Bland, G. Faini, U. Rüdiger, C. A. F. Vaz, L. Vila, and C. Vouille, Phys. Rev. Lett. **95**, 026601 (2005).
[9] G. S. D. Beach, C. Knutson, C. Nistor, M. Tsoi, and J. L. Erskine, Phys. Rev. Lett. **97**, 057203 (2006).
[10] M. Hayashi, L. Tomas, C. Rettner, R. Moriya, and S. S. P. Parkin, Nat. Phys. **3**, 21 (2007).
[11] S. S. P. Parkin, U.S. Patent No. 6,834,005 (21 December 2004); U.S. Patent No. 6,898,132 (24 May 2005); U.S. Patent No. 6,920,062 (19 July 2005); U.S. Patent No. 7,031,178 (18 April 2006); U.S. Patent No. 7,236,386 (26 June 2007); S. S. P. Parkin, M. Hayashi, and L. Thomas, Science **320**, 190 (2008).
[12] M. Tsoi, R. E. Fontana, and S. S. P. Parkin, Appl. Phys. Lett. **83**, 2617 (2003).
[13] J. Grollier, P. Boulenc, V. Cros, A. Hamzić, A. Vaurès, A. Fert, and G. Faini, Appl. Phys. Lett. **83**, 509 (2003).
[14] D. A. Allwood, G. Xiong, C. C. Faulkner, D. Atkinson, D. Petit, and R. P. Cowburn, Science **309**, 1688 (2005).
[15] N. L. Schryer and L. R. Walker, J. Appl. Phys. **45**, 5406 (1974).
[16] A. Thiaville, Y. Nakatani, J. Miltat, and N. Vernier, J. Appl. Phys. **95**, 7049 (2004).
[17] J.-Y. Lee, K.-S. Lee, S. Choi, K. Yu. Guslienko, and S.-K. Kim, Phys. Rev. B **76**, 184408 (2007).
[18] O. A. Tretiakov, D. Clarke, G.-W. Chern, Ya. B. Bazaliy, and O. Tchernyshyov, Phys. Rev. Lett. **100**, 127204 (2008).
[19] D. J. Clarke, O. A. Tretiakov, G.-W. Chern, Y. B. Bazaliy, and O. Tchernyshyov, Phys. Rev. B **78**, 134412 (2008).
[20] K. Yu Guslienko, J.-Y. Lee, and S.-K. Kim, IEEE Trans. Magn. **44**, 3079 (2008); K. Yu. Guslienko, J.-Y. Lee, and S.-K. Kim, arXiv:0711.3680 (unpublished).
[21] S.-K. Kim, J.-Y. Lee, Y.-S. Choi, K. Yu. Guslienko, and K.-S. Lee, Appl. Phys. Lett. **93**, 052503 (2008).
[22] R. Hertel and C. M. Schneider, Phys. Rev. Lett. **97**, 177202 (2006).
[23] O. A. Tretiakov and O. Tchernyshyov, Phys. Rev. B **75**, 012408 (2007).
[24] We used the OOMMF code developed by M. J. Donahue and D. G. Porter. For details, see http://math.nist.gov/oommf
[25] L. D. Landau and E. M. Lifshitz, Phys. Z. Sowjetunion **8**, 153 (1935); T. L. Gilbert, Phys. Rev. **100**, 1243 (1955) [abstract only; full report, Armor Research Foundation Project No. A059, Supplementary Report, May 1, 1956] (unpublished).
[26] J.-Y. Lee, S. Choi, and S.-K. Kim, J. Magn. **11**, 74 (2006).
[27] J.-Y. Lee, K.-S. Lee, and S.-K. Kim, Appl. Phys. Lett. **91**, 122513 (2007).
[28] It is obvious that the VW moves backward first and then forward in the longitudinal direction in a potential well with respect to the width direction, and hence resulting in a parabolic trajectory of vortex motion under an applied field. See Refs. 17 and 20.
[29] K. Yu. Guslienko, Appl. Phys. Lett. **89**, 022510 (2006); N. A. Usov and S. E. Peschany, J. Magn. Magn. Mater. **118**, L290 (1993).
[30] K. Yu. Guslienko, W. Scholz, R. W. Chantrell, and V. Novosad, Phys. Rev. B **71**, 144407 (2005).
[31] When the step-pulse field is off ($H=0$), upon the nucleation of a VC, the forward motion of the TW turns into the backward motion of the VC along the equipotential straight line (See the solid line in Fig. 4).
[32] A. Kunz and S. C. Reiff, Appl. Phys. Lett. **93**, 082503 (2008).